Parameters of the subthreshold fission structure in ^{240}Pu†

George F. Auchampaugh
Los Alamos Scientific Laboratory, Los Alamos, New Mexico 87545

Lawrence W. Weston
Holifield National Laboratory, Oak Ridge, Tennessee 37830

(Received 23 July 1975)

The neutron subthreshold fission cross section of ^{240}Pu has been measured from 500 to 10000 eV using the Oak Ridge electron linear accelerator neutron facility. A total of 82 fission widths were obtained from area and shape analysis of those resonances which define the class II states at $\cong 782$, $\cong 1405$, $\cong 1936$, and $\cong 2700$ eV. The average square of the coupling matrix element for the first three class II states is 1.85 ± 1.43 eV^2 [standard deviation (SD)]. The average class II fission width is 2.5 ± 1.0 eV (SD). Approximately 22 clusters of class I resonances were observed below 10 keV, which results in a value of 450 ± 50 eV for the average class II level spacing. Assuming parabolic inner and outer barriers, the following barrier parameters were obtained: $V_A - B_n/\hbar\omega_A = 0.71^{+0.21}_{-0.09}$ and $V_B - B_n/\hbar\omega_B = 0.53^{+0.09}_{-0.06}$.

[NUCLEAR REACTIONS ^{240}Pu(n,f); 500 to 10 000 eV; $\Gamma_{f\lambda'}$, $\Gamma^{II}_{f\lambda''}$, $\langle H_{\lambda'\lambda''}{}^2\rangle$.]

I. INTRODUCTION

The existence of narrow intermediate structure is a well-known feature in the subthreshold region of the neutron-induced fission cross sections of nuclei in the mass region $234 \leq A \leq 244$.[1-3] Lynn[4] and Weigmann[5] ascribe the observed intermediate structure to coupling between the compound nuclear states corresponding to the ground-state deformation of the nucleus "class I," and the "class II" states in the secondary minimum of the double-humped fission barrier.[6] The separation between the clusters of strong fission resonances ($D_{II} \gg D_I$) provides information on the level density of states in the secondary minimum. A detailed analysis of the structure within each cluster provides information on the coupling matrix elements $H_{\lambda'\lambda''}$ between the class II state λ'' and the class I states λ', and on the fission width $\Gamma^{II}_{f\lambda''}$, of the class II state. The average $\langle\langle H_{\lambda'\lambda''}{}^2\rangle_I\rangle_{II}$ over many class I states (denoted by $\langle\ \rangle_I$ for a fixed λ'') and the average $\langle\Gamma^{II}_{f''}\rangle_{II}$ over class II states (denoted by $\langle\ \rangle_{II}$) can be related to the penetrabilities through the inner and outer barriers, respectively.

According to Lynn,[4] the $H_{\lambda'\lambda''}{}^2$ for the λ'' state will fluctuate according to a Porter-Thomas distribution.[7] Also, $\langle H_{\lambda'\lambda''}{}^2\rangle_I$ and $\Gamma^{II}_{f\lambda''}$ will fluctuate strongly from one state to another. Therefore, to study the coupling mechanism for a given nucleus requires measuring a large number of $H_{\lambda'\lambda''}{}^2$ and $\Gamma^{II}_{f\lambda''}$.

We report in this paper on a measurement of the subthreshold neutron-induced fission cross section of ^{240}Pu and on the analysis of the intermediate structure of the first three class II states in the system ^{240}Pu + n.

II. EXPERIMENTAL DETAILS

For the ^{240}Pu(n,f) measurement the Oak Ridge Electron Linear Accelerator was operated at power levels up to 25 kW for 8-ns-wide pulses at a repetition rate of 1000 pulses per sec. A 20.0-m flight path was used for the measurement. The collimation system for this flight path was designed to view the entire ORELA neutron-producing target (Ta plus moderator) and to restrict the diameter of the neutron beam at the sample position to approximately 9.5 cm. A copper shadow bar was inserted downstream from the Ta target to shield the sample from the intense γ-ray flash associated with the $(e,\gamma;\ \gamma,n)$ reactions in the Ta target.

Data were taken on samples of ^{240}Pu, ^{239}Pu, and ^{238}U. The pressed sample of ^{240}Pu was made from a mixture of approximately 12 g of S and 10.23 g of PuO_2 (98.47% isotopic enrichment), and the metal alloy sample of ^{239}Pu from a mixture of 5.33 g of Pu (98.91%) metal and 1.07% by weight aluminum. The ^{238}U (99.99%) sample was in metallic form. The diameter of the samples was 7.62 cm. The samples were oriented at 45° to the incident neutron beam direction. At 45° they had atom/b thicknesses of 0.000 692 (^{240}Pu), 0.000 409 (^{239}Pu), and 0.00738 (^{238}U).

Two NE-213 liquid scintillators (10 cm in diameter by 5 cm thick) mounted on 12.7-cm-diam photomultipliers (58 AVP) were used as fission-neutron detectors. They were aligned perpendic-

ular to the neutron beam direction, diametrically opposite each other, about 6.5 cm from the center of the sample. A 1.3-cm-thick disk of Pb was inserted in front of each detector to reduce the intensity of the γ rays from the natural radioactivity of the sample and from γ rays which were created in the Ta target by the electron pulse and Compton scattered from the sample.

The efficiency for detecting a fission event by counting fission neutrons was about 5.0% per detector. This efficiency was determined by counting fission neutrons from the spontaneous fission of ^{240}Pu using 1.4×10^{11} y [8] for the spontaneous fission half-life. The neutron bias window was set for ~0.9- to ~5.5-MeV neutrons. The neutron efficiency was low enough to suppress effects due to multiple neutron detection, as evidenced by the fact that the ratio of coincidence to single events between the two detectors was less than 1%.

Pulse-shape discrimination (PSD) of the type developed by Forte[9] was used on the signals from each detector. An n,γ discrimination ratio of 170:1 for a capture spectrum was measured for ^{238}U.

Four tag or routing bits were generated from the outputs of the two PSD circuits: neutron detector 1, neutron detector 2, γ-ray detector 1 OR 2, and neutron detector 1 AND 2 (coincidence time ~100 ns). These tag bits allowed the neutron time-of-flight (TOF) spectra from each detector, the coincidence TOF spectrum, and the γ-ray TOF spectrum from both detectors to be accumulated simultaneously in the Oak Ridge SEL 810B data acquisition computer system.

The data presented herein were taken with channel widths of 16 ns (500 to 1300 eV) and 8 ns (1300 to 10 000 eV).

The measurement of the neutron spectrum shape was made using a ^{10}B parallel plate ionization chamber inserted in the neutron beam upstream of the sample position. The diameter of the ^{10}B deposit was 7.62 cm.

III. DATA REDUCTION

The data rate during the measurement was high enough that it was necessary to correct the TOF spectra for a system dead time of 32 μs. This correction varied from approximately 3% at 100 eV increasing to about 14% at 2 keV, and then decreasing to approximately 7% at 10 keV.

The neutron TOF spectrum contained a γ-ray background caused by γ rays that were mistagged as neutrons in the PSD circuit. This background was removed from the data by subtracting from the neutron TOF spectrum a fraction K of the corresponding γ-ray TOF spectrum. K was determined from the ratios of resonance areas in the γ-ray TOF spectrum to the corresponding areas in the neutron TOF spectrum for 20 capture resonances in ^{238}U (10 to 500 eV) and for 6 assumed capture-only resonances in ^{240}Pu (40 to 140 eV). The two values of K agreed within the errors calculated for each K, which implied that the detectors were not sensitive to the differences between the ^{238}U capture γ-ray spectrum and the ^{240}Pu capture plus fission γ-ray spectra. The effect this background had on the determination of the fission widths of weak resonances was less than 10%.

The ^{10}B data were corrected for neutron background using the 2.85-keV resonance in Na. The background measured at this energy was less than 1% of the open-beam spectrum and was assumed to be independent of energy at least over the interval of analysis (500 to 10 000 eV).

The ^{240}Pu neutron data were converted to a fission cross section by normalizing to the ^{239}Pu fission cross section[10] in the interval from 600 to 1000 eV. This normalization is described by the following equation:

$$M_s\sigma_f = \frac{N_c^{240}}{N^{10}\sqrt{E}}\langle\sigma_f\sqrt{E}\rangle^{239}\frac{\sum N^{10}}{\sum N_c^{239}}\frac{A^{240}}{A^{239}}\frac{M^{239}}{M^{240}}\frac{\epsilon_n^{239}}{\epsilon_n^{240}}, \tag{1}$$

where $i=239$ or 240; N_c^i is the neutron counts per channel corrected for mistagged γ-ray events; N^{10} is the ^{10}B neutron counts per channel; A^i is the atomic weight; M^i is the isotopic weight of the sample; ϵ_n^i is the fission neutron detection efficiency; M_s is the multiple scattering and self-shielding term; $\langle\ \rangle$ is the average from 600 to 1000 eV; $\sum$ is the sum from 600 to 1000 eV.

If we assume that $\epsilon_n^{240}\cong\epsilon_n^{239}$ ($\nu_n^{240}\cong\nu_n^{239}$) and use for $\langle\sigma_f\sqrt{E}\rangle$ 166.0 BeV$^{1/2}$, Eq. (1) becomes

$$\sigma_f = 1.24\pm 0.01(\text{stat.})\,\frac{N^{240}}{N^{10}\sqrt{E}}\ \text{(b)}, \tag{2}$$

where N^{240} represents a sum of all singles and coincidence ^{240}Pu data from both detectors.

The correction to the areas of the resonances for multiple scattering and self-shielding is only a few percent, even for those resonances with large neutron widths. Therefore M_s has been set equal to one in Eq. (2) and ignored in the subsequent analysis.

IV. RESULTS AND ANALYSIS

A. Class I parameters

The measured ^{240}Pu fission cross section from 600 to 10 000 eV is shown in Fig. 1. The high

density of points (~12 000) plotted for this interval accounts for the apparent smooth curve through the data. Below about 2 keV our energy resolution is sufficient to completely resolve the class II states into their fine-structure components (class I), as shown in Figs. 1(a)–1(c) for the states at 782, 1405, and 1936 eV. The effects of energy resolution become important for the fourth class II state at 2700 eV, where resonances observed in the total cross section[11] are not resolved in our data. For this reason, the data above 3 keV are plotted on a compressed energy scale. The structure in Figs. 1(e)–1(f) represents envelopes of class I resonances comprising the class II states. Approximately 22 clusters of class I resonances are visible below 10 keV. The average class II level spacing D_{II} is therefore 450± 50 eV. The uncertainty is calculated from the Wigner surmise[12] $[(0.27D^2/N)^{1/2}]$.

The results of an area and shape analysis of these data are presented in Table I. The thin sample approximation was used to obtain the unlabeled fission widths for an assumed constant capture width of 23.2 meV.[13] The neutron widths in the columns labeled a were taken from the total cross-section measurement of Kolar and Böckhoff.[11] The errors given for the fission widths reflect the statistical errors on the fission areas and the errors on the neutron widths.

The parameters labeled b in Table I were obtained from a shape fit to the data using the multilevel least-squares shape fitting code MULTI.[14] Even though our resolution width in the kilovolt energy region is much larger than the average total widths of the resonances in this region, a shape fit is meaningful for the strongest fission resonances. The observed widths of these resonances are greater than the resolution width, particularly for the 782-eV resonance, which has an observed width of approximately 1.3 times the resolution width. This means that either the 782-eV resonance is a doublet or is a single resonance with a very large fission width ($\Gamma_n \cong 0$). Since only one resonance has been seen at this energy, the fission width of the 782-eV resonance must therefore be on the order of the resolution width, or approximately 2 eV.

In fitting these data we used for the resolution function a convolution of a Gaussian and an exponential with e-folding widths (eV) of $1.23E$ (keV) and $1.11E$ (keV), respectively. These parameters were determined by fitting the shapes of small fission width resonances with this functional form.

Single-channel multilevel fits to the regions in the vicinity of the strongest fission resonances for the first three class II states are shown in Fig. 2. The neutron widths of the strongest fission resonances were allowed to vary. Our final values of the neutron widths agreed, within the quoted errors, with those reported by Kolar and Böckhoff.[11] To account for the apparent high background between the 791- and 811-eV resonances it was necessary to have constructive interference between these two resonances and destructive interference between the 791- and 782-eV resonances. The excellent fit to the two resonances at 1402 and 1409 eV required constructive interference between the two resonances. Also, a good fit could not be achieved constraining the neutron widths of these two resonances to the previously reported values.[11] The 1936-eV resonance which appeared to have most of the fission strength for the 1936-eV class II state had not been observed before. The fit shown in Fig. 2(c) required constructive interference between the 1936-eV resonance and its neighbor resonances, although an almost equally good fit could be obtained with all resonances interfering destructively with each other. For the 2700-eV cluster the resonances

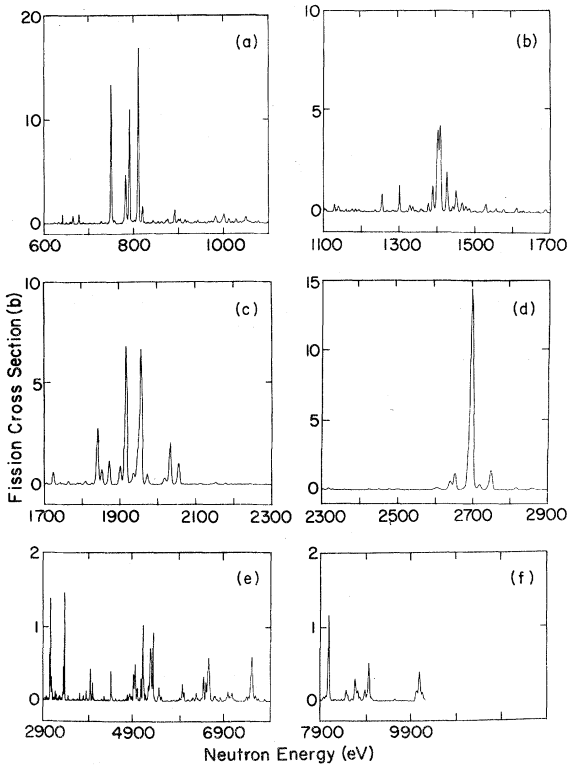

FIG. 1. ^{240}Pu subthreshold fission cross section from 500 to 10 000 eV. (a)–(d) show four class II states resolved into their fine structure components (class I). The structure in (e) and (f) represents envelopes of the fine structure of the class II states. Note the compressed energy scale for the last two figures.

were not sufficiently resolved to permit a meaningful shape fit. It also is unlikely that all the resonances in this cluster have been observed.

B. Class II resonance parameters

The plot of Γ_f vs E in Fig. 3 reveals that the widths of the envelopes of the intermediate structure are less than $D_I = 14.67$ eV.[11] This is indicated by the fact that essentially only one resonance acquires most of the class II fission width. The neutron widths given in Table I for the 782- and 1936-eV resonances are, on the average, $\sim\frac{1}{10}\langle\Gamma_n^0\rangle_{all}$; the fission widths are $\cong\Gamma_f^{II}$. (The parameters of the resonances at 1402 and 1409

TABLE I. ^{240}Pu+n class I resonance parameters.

E (eV)	Γ_n^0 [a] (meV)	Γ_f (meV)	E (eV)	Γ_n^0 [a] (meV)	Γ_f (meV)
608	0.92 ± 0.06	0.06 ± 0.05	1363	0.20 ± 0.08	$0.70^{+0.60}_{-0.20}$
632	0.53 ± 0.05	0.44 ± 0.09			
637	0.46 ± 0.05	0.17 ± 0.06	1377	1.74 ± 0.12	1.10 ± 0.10
665	7.64 ± 0.31	0.48 ± 0.05	1389	0.38 ± 0.07	5.0 ± 0.2 [b]
678	1.00 ± 0.07	0.78 ± 0.08	1402.2	0.22 ± 0.01 [b]	±2000 ± 200 [b]
712	0.050 ± 0.023	$0.80^{+0.90}_{-0.40}$	1408.5	0.23 ± 0.01 [b]	∓1500 ± 200 [b]
743	0.037 ± 0.026	$3.0^{+34.0}_{-2.4}$	1426	0.97 ± 0.10 [b]	5.3 ± 0.1 [b]
750	2.49 ± 0.12	12.70 ± 0.95	1430	0.4 ± 0.2 [b]	1.6 ± 0.3 [b]
759	0.22 ± 0.03	1.42 ± 0.59	1450	1.67 ± 0.14	3.42 ± 0.27
779	0.007 ± 0.015 [b]	10 to 100 [b]	1466	0.55 ± 0.09	2.71 ± 0.42
782.4	0.130 ± 0.002 [b]	−1450 ± 400 [b]	1484	(0.24 ± 0.08)	$1.70^{+0.80}_{-0.40}$
791.4	0.85 ± 0.05	−12.5 ± 0.4 [b]			
811.0	7.52 ± 0.35	11.6 ± 0.1 [b]	1576	3.18 ± 0.19	0.51 ± 0.06
820.3	3.84 ± 0.19	1.10 ± 0.02 [b]	1610	0.87 ± 0.10	1.12 ± 0.14
846	0.35 ± 0.03	0.93 ± 0.14	1688	0.80 ± 0.10	1.07 ± 0.15
855	1.64 ± 0.09	0.30 ± 0.05	1724	2.01 ± 0.16	2.16 ± 0.16
876	0.47 ± 0.04	0.96 ± 0.13	1742	0.60 ± 0.10	0.83 ± 0.16
891	3.16 ± 0.15	1.32 ± 0.09	1764	1.23 ± 0.11	0.65 ± 0.09
904	0.73 ± 0.05	0.67 ± 0.08	1841	2.93 ± 0.21	10.70 ± 0.74
909	2.62 ± 0.13	0.06 ± 0.04	1853	0.80 ± 0.13	4.15 ± 0.55
915	1.19 ± 0.07	0.56 ± 0.07	1873	1.79 ± 0.16	4.91 ± 0.39
943	4.00 ± 0.18	0.32 ± 0.05	1901	4.80 ± 0.29	3.0 ± 0.1 [b]
958	2.31 ± 0.16	0.19 ± 0.05	1917	0.82 ± 0.14	70.0 ± 1.0 [b]
971	2.58 ± 0.13	0.41 ± 0.05	1936	0.045 ± 0.005 [b]	−2200 ± 600 [b]
979	0.23 ± 0.05	$1.10^{+0.30}_{-0.20}$	1944	0.18 ± 0.11	1.8 ± 0.4 [b]
			1950	1.87 ± 0.17	6.3 ± 0.10 [b]
1002	3.10 ± 0.16	1.12 ± 0.08	1957	5.90 ± 0.36	25.0 ± 0.20 [b]
1042	0.39 ± 0.06	1.13 ± 0.20	1973	1.53 ± 0.17	1.80 ± 0.10 [b]
1073	3.34 ± 0.17	0.31 ± 0.05	2016	1.17 ± 0.17	2.64 ± 0.29
1099	2.54 ± 0.26	0.25 ± 0.05	2034	2.25 ± 0.21	9.79 ± 0.77
1129	1.49 ± 0.09	0.70 ± 0.08	2056	1.51 ± 0.17	5.73 ± 0.51
			2154	0.31 ± 0.15	2.28 ± 1.00
1134	0.20 ± 0.06	$0.60^{+0.3}_{-0.2}$	2178	(1.83 ± 0.18)	0.36 ± 0.07
1143	1.20 ± 0.08	0.12 ± 0.04	2577	0.94 ± 0.19	0.48 ± 0.14
1159	0.65 ± 0.06	0.28 ± 0.07	2639	8.29 ± 0.83	5.22 ± 1.29
1185	4.57 ± 0.23	0.30 ± 0.06	2652	0.71 ± 0.16	14.46 ± 2.95
1191	3.33 ± 0.17	0.34 ± 0.06	2695	6.64 ± 0.50	164 ± 18
1208	1.81 ± 0.11	0.13 ± 0.05	2719	0.78 ± 0.19	5.29 ± 0.92
1236	0.32 ± 0.06	0.59 ± 0.16	2741	3.38 ± 0.34	1.74 ± 0.35
1255	2.17 ± 0.13	1.79 ± 0.13	2750	1.95 ± 0.25	11.17 ± 1.10
1301	6.79 ± 0.35	1.47 ± 0.10	2819	0.78 ± 0.19	1.98 ± 0.36
1329	10.13 ± 0.51	0.84 ± 0.06	2845	2.94 ± 0.30	0.69 ± 0.11
1345	0.71 ± 0.08	0.47 ± 0.09	2860	0.51 ± 0.21	2.81 ± 0.85

[a] Parameters from Ref. 11.

[b] Parameters obtained from the code MULTI (Ref. 14).

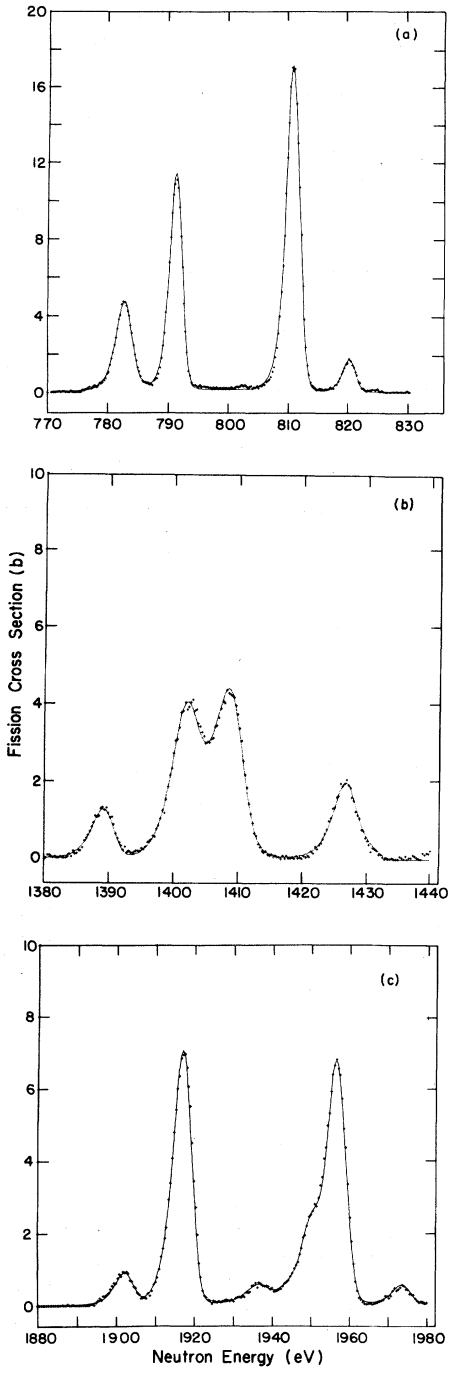

FIG. 2. Multilevel shape fits to the 782-, 1405-, and 1936-eV class II states using MULTI. Constructive interference is required between the 811- and 791-eV resonances and destructive interference between the 791- and 782-eV resonances. Constructive interference is also required between the 1402- and 1409-eV resonances. Constructive interference between the 1936-eV resonance and the neighboring resonances produces a better fit than destructive interference.

eV are not included for reasons which will be discussed in the nest section.) These two properties of the structure require that $\langle H_{\lambda'\lambda''}\rangle$ and $\langle \Gamma_f^{II}\rangle \ll D_I$. Therefore, the fission width of a class I resonance, in the uniform picket-fence model, is given by the weak mixing formula,[15]

$$\Gamma_{f\lambda'} = \frac{\langle H_{\lambda'\lambda''}{}^2\rangle\, \Gamma^{II}_{f\lambda''}}{(E_{\lambda'} - E^{II}_{\lambda''})^2 + (W/2)^2 + WD_I/2\pi} + \langle \Gamma^b_{f\lambda'}\rangle \,, \tag{3}$$

where $W = 2\pi\langle H_{\lambda'\lambda''}{}^2\rangle/D_I$ and $\langle\Gamma^b_{f\lambda'}\rangle$ is the average class I fission width for direct penetration through both barriers.

The class II fission width can be evaluated from the sum rule, $\Gamma^{II}_{f\lambda''} \cong \sum_{\lambda'}\Gamma_{f\lambda'}$; $\langle \Gamma^b_{f\lambda''}\rangle$ can be ignored since $\Gamma^{II}_{f\lambda''} \gg \langle\Gamma^b_{f\lambda''}\rangle$ (see Fig. 3).

Currently two methods are used for extracting values of $\langle H^2\rangle$ from the distribution of fission widths. One method fits the differential distribution with Eq. (3). For weak coupling, this method is sensitive to not only the strong central fission widths within each cluster, but also to the missed weak levels in the wings of the distribution. The other method, which is not as sensitive to the missed levels, fits the integral distribution,

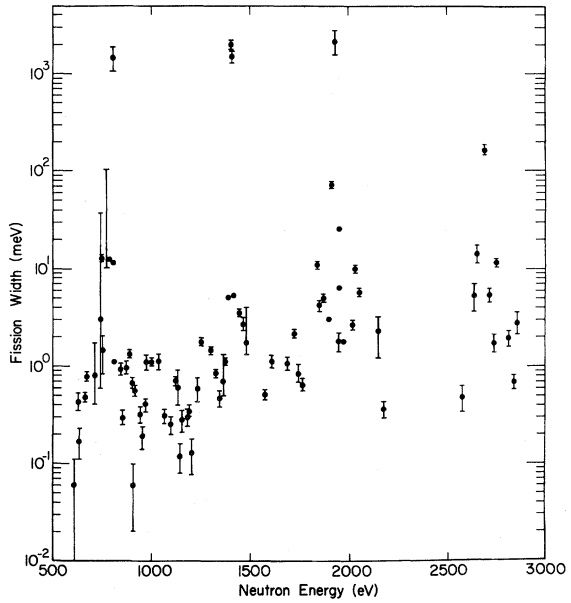

FIG. 3. Differential plot of the class I fission widths vs resonance energy. Four class II states are clearly visible at 782, 1405, 1936, and ~2700 eV. The width of each state is extremely small and much less than the class I level spacing. The apparent increase in the background fission width with energy is a consequence of poorer resolution at higher energies, and therefore a decrease in our sensitivity to weak fission strength resonances.

namely $\Sigma(E_{\lambda'})=\sum_{\lambda'}^{E_{\lambda'}}\Gamma_{f\lambda'}$ vs $E_{\lambda'}$, with the function $\bar{\Sigma}(E)=\bar{\Sigma}^b+(1/\pi)\tan^{-1}[2(E-E^{II})/W]$. This method is described in detail by Lane *et al.*[15] Regardless of which method is used to obtain values of $\langle H^2\rangle$, they are all very sensitive to the strong central fission widths and, to a lesser extent, the background term, especially for extreme weak coupling, $\langle H^2\rangle/D\ll 1$.

Since a substantial correction would have to be made for missed levels in the 1405- and 1936-eV clusters, we decided to use the integral method. We assumed that the average background fission width is equal to 0.4 ± 0.2 meV. Four fits were made to each integral distribution, allowing W and $\langle H^2\rangle$ to vary and fixing $\langle\Gamma^b\rangle$ or $\Gamma_{f\lambda''}$ (strongest fission resonance) to the following values:

$\langle\Gamma^b\rangle=0.4$,

$\langle\Gamma^b\rangle=0.6$,

$\langle\Gamma^b\rangle=0.4$

and $\Gamma_{f\lambda''}=\Gamma_{f\lambda''}+\Delta\Gamma_{f\lambda''}$ (quoted error),

$\langle\Gamma^b\rangle=$free parameter.

The results are given in Table II. The uncertainties on each $\langle H^2\rangle$ represent the largest deviation in the values of $\langle H^2\rangle$ under the four fitting conditions for each class II state. For the 1405-eV class II state it was necessary to replace the 1402- and 1409-eV resonances by a single resonance at 1405 eV with a strength equal to the sum of the strengths of the individual resonances to achieve a reasonable fit to the wings of the distribution.

V. DISCUSSION OF THE 1405-eV DOUBLET

The 1405-eV doublet represents an excellent textbook example of a near degeneracy between an unperturbed class II state E^{II} and an unperturbed class I state E^I $[(E^{II}-E^I)/2H_{12}\ll 1]$. Lynn[4] has considered this problem in detail, including the effects of the other class I resonances on the parameters of the degenerate levels. If we ignore these resonances, then the neutron widths (Γ_{ni}) and fission widths (Γ_{fi}) of the degenerate levels are equal, providing that E^{II} is equal to E^I. If E^{II} does not equal E^I, then the neutron widths and fission widths no longer are equal but satisfy the relationship,

$$\Gamma_{n1}/\Gamma_{n2}=\Gamma_{f2}/\Gamma_{f1}. \tag{4}$$

Including the other class I resonances changes the partial width parameters of the degenerate levels by an amount of the order of $\sum_{\lambda'\neq 1,2}\Gamma_{f\lambda'}/\Gamma_f^{II}$, where the sum extends over all but the degenerate levels of the class II state. Also, Eq. (4) is no longer satisfied. In our case less than 0.5% of the fission strength of the 1405-eV class II state is coupled to the other class I resonances. Therefore, the 1405-eV doublet can be treated as a simple degenerate system. The equations describing this two-level system, assuming that the class II state has no neutron width ($\Gamma_n^{II}=0$) and that the class I state has no fission width ($\Gamma_f^I=0$), are

$$E_i=\tfrac{1}{2}\{(E^{II}+E^I)\pm[(E^{II}-E^I)^2+4H_{12}^2]^{1/2}\}, \tag{5a}$$

$$\Gamma_{ni}=(C_i^I)^2\Gamma_n^I, \tag{5b}$$

$$\Gamma_{fi}=(C_i^{II})^2\Gamma_f^{II}, \tag{5c}$$

$$C_i^I=-H_{12}C_i^{II}/(E^I-E_i), \tag{5d}$$

$$(C_i^I)^2+(C_i^{II})^2=1, \tag{5e}$$

where the roman numerals denote the unperturbed parameters and the arabic subscripts the perturbed parameters ($i=1, 2$). For our case $\Gamma_{n1}/\Gamma_{n2}=0.87\pm 0.06$ and $\Gamma_{f2}/\Gamma_{f1}=0.75\pm 0.12$. Within the errors, these two ratios are equal. If we use the mean of these two values for the ratio, then we get for the unperturbed parameters: $E^I=1405.0$ eV, $E^{II}=1405.7$ eV, $\Gamma_n^I=0.45$ meV, $\Gamma_f^{II}=3500$ meV, and $H_{12}=3.13$ eV.

Equation (4) can be used to show that the sign of the level-level interference term in the cross section is negative. This means that the two resonances will interfere so that the cross section is enhanced in the region between them and diminished in the wings. Our R-matrix fit to the doublet data agrees with this prediction.

It is interesting to note that in the degenerate case (weak mixing) neither Γ_{n1} nor Γ_{n2} are necessarily small; since $(C_i^I)^2\cong\frac{1}{2}$, if Γ_n^I is large both Γ_{n1} and Γ_{n2} will be large. However, in the

TABLE II. ^{240}Pu+n class II resonance parameters.

E (eV)	$\langle H_{\lambda'\lambda''}^2\rangle_I$ (eV^2)	$\Gamma^{\downarrow}$ (eV)	$\Gamma^{\uparrow}$ (eV)
782	2.0 ± 0.4	0.86 ± 0.17	1.6 ± 0.4
1405	0.35 ± 0.30	0.15 ± 0.13	3.5 ± 0.4
1936	3.2 ± 0.6	1.37 ± 0.26	2.3 ± 0.6
	1.85 ± 1.43 (S.D.)	0.79 ± 0.61 (S.D.)	2.5 ± 1.0 (S.D.)

nondegenerate case, the resonance with essentially all the class II fission width $[(C_i^{II})^2 \cong 1]$ has a very small neutron width. This is so, not because Γ_n^I is necessarily small, but because the admixture coefficients are normalized $[(C_i^I)^2 = 1 - (C_i^{II})^2 \cong 0]$. Therefore, we cannot, in general, conclude that in weak mixing, resonances with large fission widths have smaller than average neutron widths, particularly when, as in ^{240}Pu, the probability for observing a near degeneracy is rather high, approximately 20% $(\langle 2H_{12}/(E^{II} - E^I)\rangle_{II} \sim 2(\langle\langle H_{\lambda'\lambda''}{}^2\rangle_I\rangle_{II})^{1/2}/D_I \sim 0.2)$.

It may appear that the value of $H_{12}{}^2$ calculated from the splitting of the 1405-eV doublet resonance is highly improbable for a distribution with an average $\langle H_{\lambda''}{}^2\rangle = 0.35$ eV^2. In fact, the probability of observing an $H_{\lambda'\lambda''}{}^2 \geq 9.80$ eV^2 from such a distribution is less than 10^{-5}. However, we must remember that we are observing for a particular class II state λ'' only one of the many possible distributions of $\Gamma_{f\lambda''}$ for a given ensemble $\langle H_{e\lambda''}{}^2\rangle$ and that only in moderate coupling would we expect the measured $\langle H_{\lambda''}{}^2\rangle$ to be approximately equal to $\langle H_{e\lambda''}{}^2\rangle$. To put this more clearly, if we generate many mock distributions of $H_{\lambda'\lambda''}{}^2$, or equivalently $\Gamma_{f\lambda''}$, for an $\langle H_{e\lambda''}{}^2\rangle/D \ll 1$ we find a very large variance in the values of $\langle H_{\lambda''}{}^2\rangle$ obtained from fitting each distribution separately with the function $\bar{\Sigma}(E)$.[15] In particular, for the 1405-eV state the probability of generating a distribution with an $\langle H_{\lambda''}{}^2\rangle$ of less than 0.35 eV^2 for an $\langle H_{e\lambda''}{}^2\rangle = 1.85$ eV^2 is significant and equal to ~10%. Therefore, the true ensemble $\langle H_{e\lambda''}{}^2\rangle$ for the 1405-eV state is probably much greater than 0.35 eV^2, and maybe more like several eV^2, in which case the probability of selecting an $H_{\lambda'\lambda''}{}^2 \geq 9.80$ eV^2 is more like a few percent.

VI. FISSION BARRIER PARAMETERS

The average values of $\langle\Gamma^\uparrow\rangle \equiv \Gamma_{f\lambda}^{II}$ and $\langle\Gamma^\downarrow\rangle \equiv 2\pi\langle H_{\lambda'\lambda''}{}^2\rangle/D_I$ can be related to the penetrabilities through the inner and outer barriers, respectively. If we describe these barriers by parabolas, then the heights of the inner V_A and outer V_B barriers are given by the following formulas:

$$2\pi\frac{\langle\Gamma^\uparrow\rangle}{D_{II}} = \left\{1 + \exp\left[\frac{2\pi}{\hbar\omega_A}(V_A - B_n)\right]\right\}^{-1},$$

$$2\pi\frac{\langle\Gamma^\downarrow\rangle}{D_{II}} = \left\{1 + \exp\left[\frac{2\pi}{\hbar\omega_B}(V_B - B_n)\right]\right\}^{-1}, \quad (6)$$

where B_n is the neutron binding energy and $\hbar\omega_{A,B}$ the curvature parameters of the barriers. The inner and outer barrier heights given in Table III are calculated using reported values of $\hbar\omega_{A,B}$.[16] The agreement between V_A and V_B of Ref. 16 and our values is remarkable considering that we are dealing with an s-wave barrier and they are dealing with an average over many angular momentum barriers.

The energy difference between the ground state deformation minimum and the secondary minimum of the double-humped fission barrier V_{II} given in Table III is calculated from the formula[17]

$$\frac{D_I}{D_{II}} = \left(\frac{B_n}{B_n - V_{II}}\right)^{5/4} \exp\{0.56A^{1/2}[(B_n - V_{II})^{1/2} - B_n{}^{1/2}]\} \quad (7)$$

which is based on the Fermi gas model of the nucleus.

The WKB method can be used to obtain an expression for the minimum fission width for direct penetration through both barriers of the double-humped fission barrier. Gai *et al.*[18] have shown that the minimum fission width is related to the penetrabilities through the inner and outer barriers: $\Gamma_{min} = (D_I P_A P_B)/8\pi = \frac{1}{2}\pi(\Gamma^\uparrow\Gamma^\downarrow/D_{II}{}^2)D_I$. Using our values for the parameters we get 0.22 ±0.17 meV, which is not too dissimilar from our assumed value of 0.4 ± 0.2 meV.

ACKNOWLEDGMENT

We would like to acknowledge the assistance provided by J. H. Todd of the Holifield National Laboratory in maintaining the electronic equipment during the experiment, to John D. Moses of the Los Alamos Scientific Laboratory in the analysis of the coupling matrix element distributions, and to the ORELA operations staff.

TABLE III. Inner and outer barrier heights.

^{240}Pu+n barrier parameters
$B_n = 5.24$ MeV
$V_{II} = 1.89 \pm 0.08$ MeV
Inner barrier
$\langle\Gamma^\downarrow\rangle = 0.79 \pm 0.61$ eV
$V_A - B_n/\hbar\omega_A = 0.71^{+0.21}_{-0.09}$
$V_A = 6.02^{+0.23}_{-0.10}$ MeV
$\hbar\omega_A = 1.10 \pm 0.10$ MeV [a]
$V_A = 6.25 \pm 0.20$ MeV [a]
Outer barrier
$\langle\Gamma^\downarrow\rangle = 2.5 \pm 1.0$ eV
$V_B - B_n/\hbar\omega_B = 0.53^{+0.09}_{-0.06}$
$V_B = 5.53^{+0.05}_{-0.03}$ MeV
$\hbar\omega_B = 0.55$ MeV [a]
$V_B = 5.50$ MeV [a]

[a] Parameters from Ref. 16.

† Work done under the auspices of the U. S. Energy Research and Development Administration.

[1]E. Migneco and J. P. Theobald, Nucl. Phys. A112, 603 (1968).

[2]D. Paya, H. Derrien, A. Fubini, A. Michaudon, and P. Ribon, *Nuclear Data for Reactors* (IAEA, Vienna, 1968), Vol. II, p. 128.

[3]G. D. James, Nucl. Phys. A123, 24 (1969).

[4]J. E. Lynn, United Kingdom Atomic Energy Research Establishment Report No. AERE-R 5891, 1968 (unpublished).

[5]H. Weigmann, Z. Phys. 214, 7 (1968).

[6]V. M. Strutinsky, Nucl. Phys. A95, 420 (1967).

[7]C. E. Porter and R. G. Thomas, Phys. Rev. 104, 483 (1956).

[8]C. M. Lederer, J. M. Hollander, and I. Perlman, *Table of Isotopes* (Wiley, New York, 1967), 6th ed.

[9]M. Forte, in *Proceedings of the Second United Nations International Conference on Peaceful Uses of Atomic Energy* (United Nations, Geneva, Switzerland, 1958), paper No. A/Conf. 15/P/1514.

[10]ENDF/B-IV MAT 1264, 1974 (unpublished).

[11]W. Kolar and K. H. Böckhoff, J. Nucl. Energy 22, 299 (1968).

[12]E. P. Wigner, in Proceedings of the Conference on Neutron Physics by Time-of-Flight, Gatlinburg, Tennessee, 1956 [Oak Ridge National Laboratory Report No. ORNL-2309 (unpublished)].

[13]H. Weigmann and H. Schmid, J. Nucl. Energy 22, 317 (1968).

[14]G. F. Auchampaugh, Los Alamos Scientific Laboratory Report No. LA-5473-MS, 1974 (unpublished).

[15]A. M. Lane, J. E. Lynn, and J. D. Moses, Nucl. Phys. A232, 189 (1974).

[16]B. B. Back, H. C. Britt, O. Hansen, and B. Lerous, Phys. Rev. C 10, 1948 (1974).

[17]J. E. Lynn, *The Theory of Neutron Resonance Reactions* (Clarendon, Oxford, 1968).

[18]E. V. Gai, A. V. Ignatuk, N. S. Rabotnov, and G. N. Smirenkin, in *Proceedings of the Second International Symposium on the Physics and Chemistry of Fission, Vienna, Austria, 1969* (IAEA, Vienna, 1969), paper No. SM/122/132.